

Switching nonparametric regression models for multi-curve data

Camila P. E. de Souza,^{1,2*} Nancy E. Heckman^{3*}
and Fan Xu^{4*}

¹*Department of Pathology and Laboratory Medicine, University of British Columbia, Vancouver, Canada*

²*Department of Molecular Oncology, BC Cancer Agency, Vancouver, Canada*

³*Department of Statistics, University of British Columbia, Vancouver, Canada*

⁴*Department of Industrial Engineering and Operations Research, Columbia University, New York, United States*

e-mail: desouzacpe@gmail.com

Abstract: We develop and apply an approach for analyzing multi-curve data where each curve is driven by a latent state process. The state at any particular point determines a smooth function, forcing the individual curve to “switch” from one function to another. Thus each curve follows what we call a switching nonparametric regression model. We develop an EM algorithm to estimate the model parameters. We also obtain standard errors for the parameter estimates of the state process. We consider three types of hidden states, those that are independent and identically distributed, those that follow a Markov structure and those that are independent but with distribution depending on some covariate(s). A simulation study shows the frequentist properties of our estimates. We apply our methods to a building’s power usage data.

Keywords and phrases: EM algorithm, functional data analysis, latent variables, machine learning, nonparametric regression, power usage, switching nonparametric regression model.

1. Introduction

We develop and apply a method for analyzing multi-curve data where each curve follows a *switching nonparametric regression model* (De Souza and Heckman, 2014). That is, each curve, over its domain, switches among J unobserved states with each state determining a function. The main goal is to estimate the function corresponding to each state and the parameters of the latent process, along with some measure of accuracy.

We are motivated by the problem of calculating a building’s “typical curve” of energy consumption, that is, its expected energy consumption as a function of time and other variables (e.g., weather conditions). Such knowledge allows building managers to compare the building’s real-time performance to its “typical” performance which is useful, for instance, for assessing the impact of improvements on a building’s energy efficiency. The data set we analyze was provided by PulseEnergy, now part of EnerNOC (www.enernoc.com).

*Research supported by the National Science and Engineering Research Council of Canada.

To understand our methodological approach, compare the plots in Figure 1. Figure 1a shows hourly power usage during the months of June and July 2009 in an office building. On some days (holidays and weekends) energy usage is close to zero. We observe that on some business days the energy usage is very high, approximately twice as much as on the other days. This high power consumption occurs on warm days, when the cooling system (also called the chiller) of the building was probably on. Figure 1b presents the building daytime power usage from 9am to 4pm for 44 business days in June and July 2009. Several types of curves can be observed: one type corresponds to days when the cooling system was probably on and another type when the cooling system was off. We also observe that on some days the chiller turned on in the middle of the day. On one day the chiller went on, off and then on again.

Brown, Barrington-Leigh and Brown (2012) consider the data in Figure 1a using a very computer intensive method. They find the “typical curve” by applying a local constant kernel smoother over an extremely large number of data points, and thus, their contribution to the analysis is mainly on improving computational efficiency. They do not consider the special structure we see in Figure 1b. One shortfall of their smoothing method is that they do not model the abrupt changes in level of energy consumption, and thus their approach may oversmooth these changes. Since these changes are real features of the data, they should be modelled explicitly to better understand power usage. Our method exploits the structure of Figure 1b and differs from the approach proposed by Brown, Barrington-Leigh and Brown (2012) in two important ways: by treating each business day as a replicate; and by modelling abrupt changes in the building’s power usage as arising from two functions, one function giving power usage when the chiller is off, the other function giving power usage when the chiller is on. The condition “chiller on”/“off” at any particular time is not recorded by the automatic monitoring system. Thus, it can only be inferred from the data, and so the state of the chiller forms a latent process.

De Souza and Heckman (2014) present the case where there is a single realization, a single curve switching among J functions. In that paper, we consider two models for the latent process: one where the states are independent and identically distributed, the other where the sequence of states forms a Markov chain. In addition to estimating all parameters and functions, we derive standard errors for the parameters of the latent process. In the present paper, we extend our 2014 approach into the realm of functional data analysis (Ramsay and Silverman, 2005): we consider the case when there are N curves, called replicates, with each replicate switching among J functions. This is the first work to consider the mixture of multiple functions in functional data analysis. We also consider a third type of latent state process, where the state depends on a time-varying covariate. In our application, the covariate is temperature recorded at a weather station several kilometres from the building. Preliminary data analysis indicates this dependence can be modelled via logistic regression.

Several authors have considered the single realization case from a Bayesian perspective with the smooth functions modeled as realizations of Gaussian processes. See, for instance, Tresp (2001), Rasmussen and Ghahramani (2002) and

Ou and Martin (2008). The paper of Ou and Martin (2008) also contains a Bayesian analysis of the replicate case. These papers are discussed in more detail in De Souza and Heckman (2014) and contain methodology that can, in principle, lead to estimation of all J functions and the latent variable process parameters. However, unlike our work, the focus is on the estimation of just one function - the mixture, that is, a weighted average of the J functions.

In a more recent related work, Langrock et al. (2017) consider generalized additive models with a time component, where the predictor is subject to regime changes controlled by an underlying Markov process. The parameter estimates are obtained by a numerical maximum penalized likelihood approach. The authors focus on a single realization case and do not consider the replicate case.

This paper is organized as follows. In Section 2 we provide an overview of the proposed methodology. The solution to the estimation problem is described in Section 3. Some of the calculations are similar to those that appear in De Souza and Heckman (2014); these calculations are given in the Supplementary Material. In Section 4 we present the results of a simulation study. An application of the proposed methodology to a building's power usage data is presented in Section 5. Some discussion is provided in Section 6.

The computing code and the data are available as supplementary material for possible use by interested readers.

2. Overview of the proposed methodology

We consider a data set with N replicates where replicate k contains n observations y_{1k}, \dots, y_{nk} and evaluation points x_1, \dots, x_n , which for simplicity are the same across replicates. Observation y_{ik} depends on x_i according to a hidden (unobserved) state z_{ik} with possible state values in $\{1, \dots, J\}$. If $z_{ik} = j$ the expected response of y_{ik} is $f_j(x_i)$. In this work, we assume the replicates are all generated from just one set of functions f_1, \dots, f_J , a reasonable assumption for the power usage data presented in Figure 1b and described in Section 1. We consider three types of hidden states, those that are independent and identically distributed, those that follow a Markov structure and those that are independent but with distribution depending on some covariate(s).

In principal, the x s can differ in value and number across replicates. To proceed, we need only to modify our notation and calculations, since we will model each f_j as a linear combination of B-spline basis functions. However, in our Markov state process model, a conceptual challenge arises in interpreting transition probabilities when the x s vary from replicate to replicate.

Our notation is as follows.

- Observed data: $\mathbf{x} = (x_1, \dots, x_n)^T$, fixed across replicates; covariate vectors $\mathbf{v}_{1k}, \dots, \mathbf{v}_{nk}$; responses $\mathbf{y}^R = (\mathbf{y}_1^T, \dots, \mathbf{y}_N^T)^T$, where $\mathbf{y}_k = (y_{1k}, \dots, y_{nk})^T$.
- Hidden states: $\mathbf{z}^R = (\mathbf{z}_1^T, \dots, \mathbf{z}_N^T)^T$, where $\mathbf{z}_k = (z_{1k}, \dots, z_{nk})^T$.
- $f_j(\mathbf{x}) = (f_j(x_1), \dots, f_j(x_n))^T$ for $j = 1, \dots, J$, and $f_{\mathbf{z}_k}(\mathbf{x}) = (f_{z_{1k}}(x_1), \dots, f_{z_{nk}}(x_n))^T$.

We assume that $\mathbf{z}_1, \dots, \mathbf{z}_N$, are independent. Given the hidden states \mathbf{z}_k , $\mathbf{y}_k = f_{\mathbf{z}_k}(\mathbf{x}) + \boldsymbol{\epsilon}_k$, where $\boldsymbol{\epsilon}_1, \dots, \boldsymbol{\epsilon}_N$, are independent and $\boldsymbol{\epsilon}_k$ has a multivariate normal distribution with mean equal to the 0-vector and covariance matrix \mathbf{V} , possibly depending on \mathbf{z}_k . That is, $\boldsymbol{\epsilon}_k \sim MVN(\mathbf{0}, \mathbf{V})$. Therefore, $\mathbf{y}_1, \dots, \mathbf{y}_N$ are independent and, given the hidden states \mathbf{z}_k , $\mathbf{y}_k \sim MVN(f_{\mathbf{z}_k}(\mathbf{x}), \mathbf{V})$. Our model can be considered a functional data model. In usual functional data modeling, when there is no switching regression, the observations from the k th replicate, y_{1k}, \dots, y_{nk} , are generated from a single realization of a stochastic process (see, for instance, James, Hastie and Sugar, 2000, and Yao, Müller and Wang, 2005). In our case, for the k th replicate, the observations arise from J stochastic process realizations, f_{1k}, \dots, f_{Jk} , one for each possible state. The distribution of the k th replicate of the j th stochastic process satisfies $E(f_{jk}(x)) = f_j(x)$ with the covariance between $f_{jk}(x)$ and $f_{jk}(x^*)$ generating the covariance matrix \mathbf{V} . Thus, \mathbf{V} induces a dependence among the observations of the k th realization.

We let γ be the set containing $f_1(\mathbf{x}), \dots, f_J(\mathbf{x})$ and the parameters in \mathbf{V} . We assume that the distribution of each \mathbf{z}_k is governed by a parameter vector α . Section 2.1 presents our different choices of \mathbf{V} and α .

Our goal is to estimate $\theta \equiv \{\alpha, \gamma\}$, along with standard errors or some measure of accuracy for the parameters in α . Similar to De Souza and Heckman (2014) we obtain the parameter estimates by maximizing

$$l(\theta) \equiv \sum_{k=1}^N \log p(\mathbf{y}_k | \theta) + P(f_1, \dots, f_J, \lambda_1, \dots, \lambda_J), \quad (1)$$

where $p(\mathbf{y}_k | \theta)$ is the likelihood function based on the observed data from the k th replicate and P is a roughness penalty on the f_j s. The exact form of $P(f_1, \dots, f_J, \lambda_1, \dots, \lambda_J)$ is chosen by the user. For our work, we set

$$P(f_1, \dots, f_J, \lambda_1, \dots, \lambda_J) = - \sum_{j=1}^J \lambda_j \int [f_j''(x)]^2 dx,$$

since the integrated squared second derivative of a function is a common form of roughness penalty (Wahba, 1990). The λ_j s are the smoothing parameters, governing the weight of the penalty term. As in De Souza and Heckman (2014) one could also take a Bayesian approach by maximizing (1) with P arising from placing a Gaussian process prior on the f_j s.

The form of $\log p(\mathbf{y}_k | \theta)$ is very complicated, since it involves the distribution of the latent states \mathbf{z}_k . Therefore, we apply an Expectation-Maximization (EM) algorithm (Dempster, Laird and Rubin, 1977) to maximize (1). We can show (see, for instance, Cappé, Moulines and Rydén, 2005 and McLachlan and Krishnan, 2008) that our EM algorithm generates a sequence of estimates, $\theta^{(c)}$, $c \geq 1$, satisfying $l(\theta^{(c+1)}) \geq l(\theta^{(c)})$. One could also perform a numerical likelihood maximization as described in MacDonald (2014) and Zucchini, MacDonald and Langrock (2016).

As in the single realization case presented in De Souza and Heckman (2014) we use again the results of Louis (1982) to obtain standard errors for the estimates of the parameters of the latent state process. When the hidden states,

z_{1k}, \dots, z_{nk} , are independent and identically distributed (*iid*) we consider $J \geq 2$ possible state values. For z_{1k}, \dots, z_{nk} following a Markov structure we restrict the possible number of states to $J = 2$. We also obtain standard errors for the intercept and slope parameters for the case where $J = 2$ and z_{1k}, \dots, z_{nk} are independent with the distribution of z_{ik} depending on only one covariate. See Section 2 of the Supplementary Material for more details.

2.1. Choices of \mathbf{V} and α

We consider five models for the covariance of the residual error, \mathbf{V} : unrestricted, diagonal with either $\mathbf{V} = \sigma^2 \mathbf{I}$ or with entry (i, i) depending on the latent state, and two generated from a “random intercept” covariance structure: a *homogeneous random intercept model* and a *non-homogeneous random intercept model* with variability of the intercept depending on the value of the latent state. We usually use $\mathbf{V}_{\mathbf{z}}$ to denote models where the variability depends on the latent state. However, sometimes we omit the subscript \mathbf{z} when referring to a general \mathbf{V} . The unknown parameters in \mathbf{V} are clear for our first two models. For the third model, the parameters in $\mathbf{V}_{\mathbf{z}}$ are $\sigma_1^2, \dots, \sigma_J^2$.

For \mathbf{V} to follow a homogeneous random intercept model, let $y_{ik} = f_{z_{ik}}(x_i) + \epsilon_{ik}$. Then suppose that $\epsilon_{ik} = \delta_k + e_{ik}$, where δ_k and e_{ik} are independent for all $i = 1, \dots, n$ and $k = 1, \dots, N$, and the δ_k s are *iid* $N(0, \tau^2)$ and the e_{ik} s are *iid* $N(0, \sigma^2)$. Then \mathbf{V} will depend on only two parameters and can be written as

$$\mathbf{V} = \sigma^2(\mathbf{I} + d\mathbf{1}\mathbf{1}^T), \quad (2)$$

where \mathbf{I} is an $n \times n$ identity matrix, $\mathbf{1}$ is an n -vector of ones and $d = \tau^2/\sigma^2$.

Our data analysis (Section 5) requires the more complex covariance structure of a non-homogenous random intercept model, where the variance of the random intercept depends on the state. We define this model for the simple case, where there are $J = 2$ states. We assume that $y_{ik} = f_{z_{ik}}(x_i) + \epsilon_{z_{ik}, ik}$, where $\epsilon_{1, ik} = \delta_k + e_{ik}$ when $z_{ik} = 1$ and $\epsilon_{2, ik} = \delta_k + \vartheta_k + e_{ik}$ when $z_{ik} = 2$. In addition, δ_k , ϑ_k , and e_{ik} are independent for $i = 1, \dots, n$, and $k = 1, \dots, N$, with δ_k s *iid* $N(0, \tau_1^2)$, ϑ_k s *iid* $N(0, \tau_2^2)$ and e_{ik} s *iid* $N(0, \sigma^2)$. Therefore, the covariance matrix for the non-homogeneous random intercept model is given by

$$\mathbf{V}_{\mathbf{z}_k} = \sigma^2(\mathbf{I} + d_1\mathbf{1}\mathbf{1}^T + d_2\mathbf{1}_{\mathbf{z}_k}\mathbf{1}_{\mathbf{z}_k}^T), \quad (3)$$

where $d_j = \tau_j^2/\sigma^2$ and $\mathbf{1}_{\mathbf{z}_k}$ is an n -vector with i th entry $\mathbb{I}(z_{ik} = 2)$.

In our model α is the vector containing the parameters governing the distribution of the hidden states. If z_{1k}, \dots, z_{nk} are *iid*, then α is of length J with j th component equal to $p(z_{ik} = j|\alpha) \equiv p_j$. If z_{1k}, \dots, z_{nk} follow a Markov structure, that is, if $p(z_{ik}|z_{(i-1)k}, \dots, z_{1k}, \alpha) = p(z_{ik}|z_{(i-1)k}, \alpha)$, $i = 2, \dots, n$, then the parameter vector α consists of the initial probabilities, $\pi_j = p(z_{ik} = 1|\alpha)$, and the transition probabilities, $a_{lj} = p(z_{ik} = j|z_{(i-1)k} = l, \alpha)$, $j, l = 1, \dots, J$. Note that the transition probabilities do not depend on i or k .

In the case where z_{1k}, \dots, z_{nk} are independent, with the distribution of z_{ik} depending on a vector of covariates $\mathbf{v}_{ik} = (1, v_{1, ik}, v_{2, ik}, \dots, v_{M, ik})^T$, we assume

that $p(z_{ik} = j | \mathbf{v}_{ik}, \alpha) \equiv p_j(\mathbf{v}_{ik}, \alpha)$ follows a multinomial logistic regression model with

$$\log \frac{p_j(\mathbf{v}_{ik}, \alpha)}{p_1(\mathbf{v}_{ik}, \alpha)} = \beta_{j0} + \beta_{j1}v_{1,ik} + \cdots + \beta_{jM}v_{M,ik} = \boldsymbol{\beta}_j^T \mathbf{v}_{ik} \text{ for } j = 2, \dots, J$$

so that

$$p_1(\mathbf{v}_{ik}, \alpha) = \frac{1}{1 + \sum_{j=2}^J e^{\boldsymbol{\beta}_j^T \mathbf{v}_{ik}}}$$

and

$$p_j(\mathbf{v}_{ik}, \alpha) = \frac{e^{\boldsymbol{\beta}_j^T \mathbf{v}_{ik}}}{1 + \sum_{j=2}^J e^{\boldsymbol{\beta}_j^T \mathbf{v}_{ik}}} \text{ for } j = 2, \dots, J.$$

In this case α contains all the regression coefficient vectors $\boldsymbol{\beta}_2, \dots, \boldsymbol{\beta}_J$.

3. Parameter estimation

Here we present the proposed EM algorithm to obtain the estimates of the parameters in θ . In the M-step, we take the same approach as [De Souza and Heckman \(2014\)](#) and model each f_j as a linear combination of K known cubic B-spline basis functions, so that $f_j(\mathbf{x}) = \mathbf{B}\phi_j$, where ϕ_j is the K -vector of coefficients corresponding to f_j and \mathbf{B} is the $n \times K$ matrix with entries $B_{i\nu} = b_\nu(x_i)$.

The smoothing parameters, $\lambda_1, \dots, \lambda_J$, can be chosen by a data driven method or subjectively by visual inspection. In [Section 3.3](#), we propose and justify a leave-one-curve-out cross-validation criterion to find the optimal λ_j s for the case when \mathbf{V} is diagonal and use this method in our application. In our application, when \mathbf{V} is based on the nonhomogeneous random intercept model, we choose the smoothing parameters via a ‘‘brute force’’ leave-one-curve-out method, assuming that $\lambda_1 = \lambda_2 = \lambda$. We use a weighted cross-validation criterion where the weights reflect the uncertainty of the hidden states (see [Section 3](#) of the [Supplementary Material](#)). In all of our simulation studies, to reduce computation time, we pre-choose the λ_j s by examining a few data sets and visually ensuring that the estimated functions have the same smoothness and shape as the true curves.

Let $p(\mathbf{y}^R, \mathbf{z}^R | \theta)$ be the joint distribution of the observed and latent data given θ , also called the complete data distribution. The application of the EM algorithm to the replicate case is similar to that of the one realization case considered in [De Souza and Heckman \(2014\)](#), which is based on writing

$$\log p(\mathbf{y}^R, \mathbf{z}^R | \theta) = \log p(\mathbf{y}^R | \mathbf{z}^R, \theta) + \log p(\mathbf{z}^R | \theta) \equiv \mathcal{L}_1(\gamma) + \mathcal{L}_2(\alpha).$$

In what follows we present a summary of the E and M steps. See [Section 1](#) of the [Supplementary Material](#) for details.

In the E-step we calculate

$$Q(\theta, \theta^{(c)}) \equiv E_{\theta^{(c)}}(\log p(\mathbf{y}^R, \mathbf{z}^R | \theta) | \mathbf{y}^R) = E_{\theta^{(c)}}(\mathcal{L}_1(\gamma) | \mathbf{y}^R) + E_{\theta^{(c)}}(\mathcal{L}_2(\alpha) | \mathbf{y}^R).$$

In the M-step, we want to find $\theta^{(c+1)}$ that maximizes $S(\theta, \theta^{(c)}) \equiv Q(\theta, \theta^{(c)}) + P(f_1, \dots, f_J, \lambda_1, \dots, \lambda_J)$ with respect to θ , or at least satisfies $S(\theta^{(c+1)}, \theta^{(c)}) \geq S(\theta^{(c)}, \theta^{(c)})$. Let \mathbf{s} be an n -vector of possible hidden states, i.e., each entry of \mathbf{s} is in $\{1, 2, \dots, J\}$, and let

$$p_k(\mathbf{s})^{(c)} \equiv p(\mathbf{z}_k = \mathbf{s} | \mathbf{y}^R, \theta^{(c)}) = p(\mathbf{z}_k = \mathbf{s} | \mathbf{y}_k, \theta^{(c)}),$$

whose value depends on the model assumed for the hidden states. Therefore, disregarding the constant terms, we maximize

$$S^*(\theta, \theta^{(c)}) \equiv -\frac{1}{2} \sum_{k=1}^N \sum_{\text{all } \mathbf{s}} p_k(\mathbf{s})^{(c)} [(\mathbf{y}_k - f_{\mathbf{s}}(\mathbf{x}))^T \mathbf{V}_{\mathbf{s}}^{-1} (\mathbf{y}_k - f_{\mathbf{s}}(\mathbf{x})) + \log |\mathbf{V}_{\mathbf{s}}|] \quad (4)$$

$$+ P(f_1, \dots, f_J, \lambda_1, \dots, \lambda_J) \quad (5)$$

$$+ \sum_{k=1}^N \sum_{\text{all } \mathbf{s}} p_k(\mathbf{s})^{(c)} \log p(\mathbf{z}_k = \mathbf{s} | \alpha) \quad (6)$$

with respect to $\theta = \{\alpha, f_1(\mathbf{x}), \dots, f_J(\mathbf{x}), \text{ and the parameters in } \mathbf{V}\}$. Note that $\theta^{(c)}$ is fixed and thus so are the $p_k(\mathbf{s})^{(c)}$ s. We also consider the smoothing parameters, $\lambda_1, \dots, \lambda_J$, to be fixed. We apply a natural extension of the EM approach, the Expectation-Conditional Maximization (ECM) algorithm (Meng and Rubin, 1993), to obtain the parameter updates $\theta^{(c+1)}$.

3.1. M-step via an ECM algorithm

The steps of the ECM algorithm are summarized as follows.

1. Hold \mathbf{V} and the parameters in α fixed and maximize S^* with respect to $f_1(\mathbf{x}), \dots, f_J(\mathbf{x})$, obtaining $f_1(\mathbf{x})^{(c+1)}, \dots, f_J(\mathbf{x})^{(c+1)}$. That is, maximize the sum of (4) and (5).
2. Hold $f_1(\mathbf{x}), \dots, f_J(\mathbf{x})$ and the parameters in α fixed and maximize (4) with respect to the parameters in \mathbf{V} , obtaining $\mathbf{V}^{(c+1)}$.
3. Hold $f_1(\mathbf{x}), \dots, f_J(\mathbf{x})$ and \mathbf{V} fixed and maximize (6) with respect to the parameters in α , obtaining $\alpha^{(c+1)}$.

The results for Steps 1, 2 and 3 are given below. Details can be found in Section 1.2 of the Supplementary Material.

Step 1. *Updating $f_1(\mathbf{x}), \dots, f_J(\mathbf{x})$.*

We propose a method to update the $f_j(\mathbf{x})$ s that is straightforward and yields an estimate of $\mathbf{f} = (f_1(\mathbf{x})^T, \dots, f_J(\mathbf{x})^T)^T$ in closed form. The trick is to write $f_{\mathbf{s}}(\mathbf{x})$ in terms of $f_1(\mathbf{x}), \dots, f_J(\mathbf{x})$. To do this, let $\mathbf{1}_{j,\mathbf{s}}$ be the n -vector with i th element equal to 1 if $s_i = j$, 0 else. Let $\mathcal{I}_{\mathbf{s}}$ be the n by nJ matrix, $\mathcal{I}_{\mathbf{s}} = [\text{diag}(\mathbf{1}_{1,\mathbf{s}}) \mid \dots \mid \text{diag}(\mathbf{1}_{J,\mathbf{s}})]$. Then we easily see that $f_{\mathbf{s}}(\mathbf{x}) = \mathcal{I}_{\mathbf{s}} \mathbf{f}$. Recall that $f_j(\mathbf{x}) = \mathbf{B} \phi_j$. Let \mathbf{B}^* be the $nJ \times KJ$ block diagonal matrix with each block equal to \mathbf{B} and let ϕ be the JK -vector $\phi = (\phi_1^T, \dots, \phi_J^T)^T$. Therefore $\mathbf{f} = \mathbf{B}^* \phi$.

Let \mathbf{R} be the $K \times K$ matrix with entries $\mathbf{R}_{\nu\nu'} = \int b''_{\nu}(x)b''_{\nu'}(x) dx$. Combining these calculations we see that, to find the f_{js} that maximize the sum of (4) and (5), we must maximize, as a function of ϕ ,

$$-\frac{1}{2} \sum_{k=1}^N \sum_{\text{all } \mathbf{s}} p_k(\mathbf{s})^{(c)} [(\mathbf{y}_k - \mathcal{I}_{\mathbf{s}} \mathbf{B}^* \phi)^T \mathbf{V}_{\mathbf{s}}^{-1} (\mathbf{y}_k - \mathcal{I}_{\mathbf{s}} \mathbf{B}^* \phi)] - \phi^T \text{diag}(\lambda_1 \mathbf{R}, \dots, \lambda_J \mathbf{R}) \phi.$$

This expression is quadratic in ϕ and is easily maximized in closed form. Let $\phi^{(c+1)}$ be this maximizing ϕ when we set $\mathbf{V} = \mathbf{V}^{(c)}$. So we let $\mathbf{f}^{(c+1)} = \mathbf{B}^* \phi^{(c+1)}$.

Step 2. *Updating* \mathbf{V} .

For a model with $\mathbf{V}_{\mathbf{s}} \equiv \mathbf{V}$, with no dependence on the state vector \mathbf{s} and no restrictions on the form of \mathbf{V} , we show that $\mathbf{V}^{(c+1)}$ is

$$\widehat{\mathbf{V}} = \frac{1}{N} \sum_{k=1}^N \sum_{\text{all } \mathbf{s}} p_k(\mathbf{s})^{(c)} (\mathbf{y}_k - f_{\mathbf{s}}(\mathbf{x})) (\mathbf{y}_k - f_{\mathbf{s}}(\mathbf{x}))^T$$

with $f_{\mathbf{s}}(\mathbf{x}) = f_{\mathbf{s}}(\mathbf{x})^{(c+1)}$. Note that if the values of \mathbf{z}_k were non-random and known, then $p_k(\mathbf{s})^{(c)}$ is a delta function and so $\widehat{\mathbf{V}}$ is similar to the sample covariance matrix of the \mathbf{y}_k s.

When $\mathbf{V}_{\mathbf{s}} \equiv \mathbf{V}$ follows a homogeneous random intercept model we update the parameter estimates of the restricted \mathbf{V} in (2) as follows. Let $\sigma^{2(c+1)}$ be

$$\begin{aligned} \hat{\sigma}^2 &= \frac{1}{N(n-1)} \left(\sum_{k=1}^N \sum_{\text{all } \mathbf{s}} p_k(\mathbf{s})^{(c)} (\mathbf{y}_k - f_{\mathbf{s}}(\mathbf{x}))^T (\mathbf{y}_k - f_{\mathbf{s}}(\mathbf{x})) \right. \\ &\quad \left. - \frac{1}{n} \sum_{k=1}^N \sum_{\text{all } \mathbf{s}} p_k(\mathbf{s})^{(c)} [(\mathbf{y}_k - f_{\mathbf{s}}(\mathbf{x}))^T \mathbf{1}]^2 \right), \end{aligned}$$

and $d^{(c+1)}$ be

$$\hat{d} = \frac{1}{\sigma^2 N n^2} \sum_{k=1}^N \sum_{\text{all } \mathbf{s}} p_k(\mathbf{s})^{(c)} [(\mathbf{y}_k - f_{\mathbf{s}}(\mathbf{x}))^T \mathbf{1}]^2 - \frac{1}{n}$$

with σ^2 replaced by $\sigma^{2(c+1)}$. Therefore $\tau^{2(c+1)} = d^{(c+1)} \times \sigma^{2(c+1)}$.

The maximization in Step 2 when $\mathbf{V}_{\mathbf{s}}$ follows the non-homogeneous random intercept model is given in Section 1.2 of the Supplementary Material, for the case of $J = 2$ states. The ECM algorithm for diagonal $\mathbf{V}_{\mathbf{s}}$ is given in Section 3.2.

Step 3. *Updating* α (any \mathbf{V}).

We maximize (6) with respect to the parameters in α , with the calculations depending on the proposed model for the hidden states.

When z_{1k}, \dots, z_{nk} are *iid* with $p_j = p(z_{ik} = j | \alpha)$ we obtain

$$p_j^{(c+1)} = \frac{1}{Nn} \sum_{k=1}^N \sum_{\text{all } \mathbf{s}} p_k(\mathbf{s})^{(c)} n_{\mathbf{s},j}.$$

For Markov $z_{ik}\mathbf{s}$, where the vector α is composed of transition probabilities a_{lj} and initial probabilities π_j , we obtain

$$\pi_j^{(c+1)} = \frac{1}{N} \sum_{k=1}^N \sum_{\text{all } \mathbf{s}} p_k(\mathbf{s})^{(c)} \mathbf{I}(s_1 = j)$$

and

$$a_{lj}^{(c+1)} = \frac{\sum_{k=1}^N \sum_{\text{all } \mathbf{s}} p_k(\mathbf{s})^{(c)} n_{\mathbf{s},lj}}{\sum_{k=1}^N \sum_{\text{all } \mathbf{s}} p_k(\mathbf{s})^{(c)} \sum_{i=2}^n \mathbf{I}(s_{i-1} = l)},$$

where $n_{\mathbf{s},lj}$ is the number of transitions in \mathbf{s} from state l to state j , that is, $n_{\mathbf{s},lj} = \sum_{i=2}^n \mathbf{I}\{s_{i-1} = l, s_i = j\}$.

When z_{1k}, \dots, z_{nk} are independent with the distribution of z_{ik} depending on some covariate(s), α contains the regression coefficients from our logistic regression model for $p(z_{ik} = j | \mathbf{v}_{ik}, \alpha) \equiv p_j(\mathbf{v}_{ik}, \alpha)$. In this case, (6) becomes

$$\sum_{k=1}^N \sum_{\text{all } \mathbf{s}} p_k(\mathbf{s})^{(c)} \sum_{i=1}^n \sum_{j=1}^J \log p_j(\mathbf{v}_{ik}, \alpha) \mathbf{I}\{s_i = j\},$$

which must be maximized numerically, for instance, via a Newton-Raphson method.

3.2. ECM algorithm when \mathbf{V} is diagonal

Recall that we consider two cases of \mathbf{V} diagonal, one with $\mathbf{V} = \sigma^2 \mathbf{I}$ and one with $\mathbf{V} = \mathbf{V}_{\mathbf{z}_k} = \text{diag}(\sigma_{z_{1k}}^2, \dots, \sigma_{z_{nk}}^2)$. We could use the notation and steps of Section 3.1, modifying Step 2 for these types of \mathbf{V} . However, it is much easier to re-derive all three steps using the independence of the components of \mathbf{y}_k in order to rewrite $\mathcal{L}_1(\gamma)$, and thus $S(\theta, \theta^{(c)})$, in simpler form. We will see below that, instead of the $p_k(\mathbf{s})^{(c)}$ s in (4) and (6), we require the simpler

$$p_{ik}(j)^{(c)} = p(z_{ik} = j | \mathbf{y}_k, \theta^{(c)}).$$

The forms of $p_{ik}(j)^{(c)}$ are given in Section 1.3 of the Supplementary Material.

Here, we carry out the calculations of the ECM algorithm for the case that $\mathbf{V}_{\mathbf{z}_k} = \text{diag}(\sigma_{z_{1k}}^2, \dots, \sigma_{z_{nk}}^2)$, as they can be easily modified for the case that $\mathbf{V} = \sigma^2 \mathbf{I}$: simply replace σ_j^2 by σ^2 .

We want to find $\theta = \{f_j(\mathbf{x}), \sigma_j^2, j = 1, \dots, J, \text{ and } \alpha\}$ that maximizes

$$S^*(\theta, \theta^{(c)}) = -\frac{1}{2} \sum_{k=1}^N \sum_{i=1}^n \sum_{j=1}^J p_{1k}(j)^{(c)} \log \sigma_j^2 \quad (7)$$

$$-\frac{1}{2} \sum_{k=1}^N \sum_{j=1}^J (\mathbf{y}_k - f_j(\mathbf{x}))^T \mathbf{W}_{kj} (\mathbf{y}_k - f_j(\mathbf{x})) \quad (8)$$

$$+ P(f_1, \dots, f_J, \lambda_1, \dots, \lambda_J) \quad (9)$$

$$+ \mathbf{E}_{\theta^{(c)}}(\mathcal{L}_2(\alpha) | \mathbf{y}^R), \quad (10)$$

where

$$\mathbf{W}_{kj} = \sigma_j^{-2} \text{diag}(p_{1k}(j)^{(c)}, \dots, p_{nk}(j)^{(c)}). \quad (11)$$

We apply the ECM algorithm as follows.

1. *Updating* the $f_j(\mathbf{x})$ s. Holding the σ_j^2 s and the parameters in α fixed and maximizing the sum of (8) and (9) with respect to $f_j(\mathbf{x})$ we obtain

$$\hat{f}_j(\mathbf{x}) = \sum_{k=1}^N \mathbf{H}_{kj}(\lambda_j) \mathbf{y}_k,$$

where

$$\mathbf{H}_{kj}(\lambda) = \mathbf{B} \left(\mathbf{B}^T \sum_{r=1}^N \mathbf{W}_{rj} \mathbf{B} + 2\lambda \mathbf{R} \right)^{-1} \mathbf{B}^T \mathbf{W}_{kj}. \quad (12)$$

We let $f_j(\mathbf{x})^{(c+1)}$ be $\hat{f}_j(\mathbf{x})$ with σ_j^2 in \mathbf{W}_{kj} replaced by $\sigma_j^{2(c)}$.

2. *Updating the σ_j^2 s.* Holding the $f_j(\mathbf{x})$ s and α fixed and maximizing the sum of (7) and (8) with respect to σ_j^2 we get

$$\hat{\sigma}_j^2 = \frac{\sum_{k=1}^N \sum_{i=1}^n p_{ik}(j)^{(c)} [y_{ik} - f_j(x_i)]^2}{\sum_{k=1}^N \sum_{i=1}^n p_{ik}(j)^{(c)}}.$$

Let $\sigma_j^{2(c+1)}$ be $\hat{\sigma}_j^2$ with $f_j(x_i) = f_j(x_i)^{(c+1)}$.

3. *Updating α .* Hold the $f_j(\mathbf{x})$ s and the σ_j^2 s fixed and maximize (10) with respect to the parameters in α . For *iid* z_{iks} we obtain

$$p_j^{(c+1)} = \frac{1}{Nn} \sum_{k=1}^N \sum_{i=1}^n p_{ik}(j)^{(c)}.$$

For Markov z_{ik} s, we have

$$a_{lj}^{(c+1)} = \frac{\sum_{k=1}^N \sum_{i=2}^n p(z_{(i-1)k} = l, z_{ik} = j | \mathbf{y}_k, \theta^{(c)})}{\sum_{k=1}^N \sum_{i=2}^n p(z_{(i-1)k} = l | \mathbf{y}_k, \theta^{(c)})}$$

and

$$\pi_j^{(c+1)} = \frac{1}{N} \sum_{k=1}^N p_{1k}(j)^{(c)}.$$

For z_{ik} s independent with distribution of z_{ik} depending on some covariates we need numerical optimization methods, such as Newton-Raphson, to obtain the coefficient estimates from our logistic regression model for $p(z_{ik} = j | \mathbf{v}_{ik}, \alpha)$. So, for example, if there are $J = 2$ states and the covariate vector is $\mathbf{v}_{ik} = (1, v_{ik})^T$, we apply a numerical method to obtain β_{20} and β_{21} that maximize

$$E_{\theta^{(c)}}(\mathcal{L}_2(\beta_{20}, \beta_{21}) | \mathbf{y}^R) = \sum_{k=1}^N \sum_{i=1}^n \{p_{ik}(2)^{(c)}(\beta_{20} + \beta_{21} v_{ik}) - \log(1 + e^{\beta_{20} + \beta_{21} v_{ik}})\}.$$

3.3. Choice of the smoothing parameters when \mathbf{V} is diagonal

In principal, we can always compute the smoothing parameters by “leave-one-curve-out” cross-validation. However, for many models, this can be computationally intensive. Fortunately, in the models with $\mathbf{V} = \sigma^2 \mathbf{I}$ or $\mathbf{V}_{\mathbf{z}_k} = \text{diag}(\sigma_{z_{1k}}^2, \dots, \sigma_{z_{nk}}^2)$, we can shorten calculations by using Theorem 1 below. In this section, we describe our iterative cross-validation procedure, implemented for our data analysis in Section 5.1 for $\mathbf{V}_{\mathbf{z}_k} = \text{diag}(\sigma_{z_{1k}}^2, \dots, \sigma_{z_{nk}}^2)$. The steps for $\mathbf{V} = \sigma^2 \mathbf{I}$ are the same except with $\hat{\sigma}^2$ replacing the $\hat{\sigma}_j^2$ s.

In our data analysis we set the initial values, the $\lambda_j^{(0)}$ s, to those that worked well when tested on the data set. We update the λ_j s as follows.

1. At iteration i , with $\lambda_j = \lambda_j^{(i)}$, $j = 1, \dots, J$, use the ECM algorithm of Section 3.2 to find the $\hat{p}_{ik}(j)$ s, the $\hat{\sigma}_j^2$ s and the \hat{f}_j s.
2. Discard the \hat{f}_j s from Step 1.
3. Let $\widehat{\mathbf{W}}_{kj}$ be \mathbf{W}_{kj} as defined in (11) but with the $\hat{\sigma}_j^2$ s and $\hat{p}_{ik}(j)$ s replacing the σ_j^2 s and $p_{ik}(j)$ s. Treat the $\hat{\sigma}_j^2$ s and the $\hat{p}_{ik}(j)$ s and thus the $\widehat{\mathbf{W}}_{kj}$ s as fixed.
4. For $j = 1, \dots, J$, over a grid of possible λ values, set $\lambda_j^{(i+1)}$ as the value of λ that minimizes the following leave-one-replicate-out cross-validation criterion:

$$CV_j(\lambda) = \sum_{k=1}^N [\mathbf{y}_k - \hat{f}_{j\lambda}^{(-k)}(\mathbf{x})]^T \widehat{\mathbf{W}}_{kj} [\mathbf{y}_k - \hat{f}_{j\lambda}^{(-k)}(\mathbf{x})] \quad (13)$$

where $\hat{f}_{j\lambda}^{(-k)}$ is the function that maximizes

$$S_j^{(-k)}(f_j) = -\frac{1}{2} \sum_{r=1:r \neq k}^N [\mathbf{y}_r - f_j(\mathbf{x})]^T \widehat{\mathbf{W}}_{rj} [\mathbf{y}_r - f_j(\mathbf{x})] + P(f_j, \lambda).$$

5. Repeat steps 1-4 with $\lambda_j = \lambda_j^{(i+1)}$, $j = 1, \dots, J$, until convergence.

We use the final values of the λ_j s to obtain all of the parameter estimates from the ECM algorithm as in Section 3.2.

Finding λ that minimizes (13) is computationally intensive. Fortunately, we have the following theorem.

Theorem 1 *Let $\hat{f}_{1\lambda}, \dots, \hat{f}_{J\lambda}$ be the maximizers of the sum of (8) and (9), with \mathbf{W}_{kj} replaced by $\widehat{\mathbf{W}}_{kj}$. Let $\widehat{\mathbf{H}}_{kj}$ be as in (12), but with \mathbf{W}_{kj} replaced by $\widehat{\mathbf{W}}_{kj}$. Suppose that $\mathbf{I} - \widehat{\mathbf{H}}_{kj}$ is invertible and $\widehat{\mathbf{W}}_{kj}$ is positive definite, $j = 1, \dots, J$. Then*

$$CV_j(\lambda) = \sum_{k=1}^N \left[(\mathbf{I} - \widehat{\mathbf{H}}_{kj}(\lambda))^{-1} (\hat{f}_{j\lambda}(\mathbf{x}) - \mathbf{y}_k) \right]^T \widehat{\mathbf{W}}_{kj} \left[(\mathbf{I} - \widehat{\mathbf{H}}_{kj}(\lambda))^{-1} (\hat{f}_{j\lambda}(\mathbf{x}) - \mathbf{y}_k) \right].$$

The proof follows directly from Lemma 2 in the Appendix, which holds in a slightly more general setting.

4. Simulation study

We carry out a simulation study under three different designs considering that the hidden states, the z_{ik} s, can take values 1 or 2. For each design 300 independent data sets are generated, each with $N = 100$ replicates. In design 1, z_{1k}, \dots, z_{nk} are *iid* and \mathbf{V} follows the homogeneous random intercept model as in (2). In design 2, z_{1k}, \dots, z_{nk} follow a Markov structure and \mathbf{V} also follows the homogeneous random intercept model. In design 3, z_{1k}, \dots, z_{nk} are independent with the distribution of z_{ik} depending on a univariate covariate, v_{ik} . In this third design, we take $\mathbf{V} = \sigma^2 \mathbf{I}$. To study all three designs we use the same vector of evaluation points \mathbf{x} and the same true functions f_1 and f_2 . The vector $\mathbf{x} = (x_1, \dots, x_n)^T$ consists of $n = 10$ equally spaced points, 1, 12, 23, \dots , 89, 100. The true function f_2 is the same we used in the simulation study presented in De Souza and Heckman (2014). The true function f_1 is simply $f_2 - 0.1$. In the third study, for each simulated data set, we generate $v_{ik}, k = 1, \dots, n, i = 1, \dots, N$. Figure 2 contains example data sets generated from each of the three designs.

For Designs 1 and 2 we generate each simulated data set as follows.

1. Generate the z_{ik} s according to the specified model - *iid* for Design 1, Markov for Design 2. For the *iid* model, we set $p_1 = p(z_{ik} = 1) = 0.5$. For Markov z_{ik} s, we set transition probabilities $a_{12} = p(z_i = 2 | z_{i-1} = 1) = 0.3$ and $a_{21} = p(z_i = 1 | z_{i-1} = 2) = 0.4$ and initial probabilities $\pi_1 = \pi_2 = 0.5$.

2. Generate the y_{ik} s according to the homogeneous random intercept model of Section 2.1 with $\tau^2 = 10^{-4}$ and $\sigma^2 = 10^{-5}$.
3. Repeat steps 1 and 2 $N = 100$ times to obtain a data set of 100 replicates.

For Design 3 we generate each simulated data set as follows.

1. Generate v_{ik} s *iid* $N(0, 1)$.
2. Generate the z_{ik} s such that $p(z_{ik} = 1|v_{ik}) \equiv p_1(v_{ik}) = 1/[1 + \exp(\beta_0 + \beta_1 v_{ik})]$ and so $\log[p_2(v_{ik})/p_1(v_{ik})] = \beta_0 + \beta_1 v_{ik}$. We set $\beta_0 = 2$ and $\beta_1 = 5$.
3. Generate the y_{ik} s as follows. If $z_{ik} = 1$ then $y_{ik} = f_1(x_i) + e_{ik}$. If $z_{ik} = 2$ then $y_{ik} = f_2(x_i) + e_{ik}$. The e_{ik} s are *iid* $N(0, \sigma^2)$. We set $\sigma^2 = 5 \times 10^{-5}$.
4. Repeat steps 1, 2 and 3 $N = 100$ times to obtain a data set of 100 replicates.

We analyze the simulated data under each design using the proposed EM algorithm. We set initial parameter values to the true parameter values to speed up computation. We did try initial values that were different than the true parameter values and the EM algorithm also converged, but it took longer than when starting from the truth, as expected.

The values of λ_1 and λ_2 are fixed and equal to 10^{-4} in the study of all designs. We choose this value by examining a few simulated data sets and a range of lambda values. We find that the results of these preliminary analyses are not sensitive to the choice of smoothing parameter over a wide range of lambda values.

4.1. Results

The three plots in Figure 2 show the fitted values $\hat{f}_1(\mathbf{x})$ and $\hat{f}_2(\mathbf{x})$ (dashed curves) for a data set generated from each simulation design.

We assess the quality of the estimated functions via the pointwise empirical mean squared error (EMSE) as in De Souza and Heckman (2014). For all designs $\hat{f}_1(\mathbf{x})$ and $\hat{f}_2(\mathbf{x})$ produce very small values of EMSE ($< 2 \times 10^{-6}$). However, when generating data according to Design 3, the EMSE values for $\hat{f}_1(\mathbf{x})$ are larger than for Designs 1 and 2.

We observe that in all cases we are slightly underestimating the values of the variance parameters. This may be due to the challenges of correctly adjusting the degrees of freedom in the estimates, in order to account for the estimation of the f_j s. Recall that, in Designs 1 and 2, the error variance satisfies $10^5 \sigma^2 = 1$ and in Design 3, $10^5 \sigma^2 = 5$. The averages of our estimates of $10^5 \sigma^2$ (with standard errors) under Designs 1, 2 and 3 are, respectively, 0.978 (0.046), 0.977 (0.045) and 4.919 (0.238). In Designs 1 and 2, we have an additional variance parameter, namely, the variance of the random effect intercept, with $10^4 \tau^2 = 1$. In these cases, the averages of $10^4 \tau^2$ are equal to 0.977 with standard deviations equal to 0.152.

Table 1 contains the mean and the standard deviation of the estimates of the parameters of the latent process under each simulation design, along with the averages of our proposed standard errors (SEs). Note that the standard

deviations of the estimates are close to the values of the means of the proposed SEs, as desired. Table 1 also shows the empirical coverage percentages of a 90% and a 95% confidence interval. We consider confidence intervals of the form “mean of the parameter estimates $\pm z_{\alpha/2} \times$ proposed SE”, where $z_{\alpha/2}$ is the $\alpha/2$ quantile of a standard normal distribution with $\alpha = 0.1$ and 0.05 . The empirical coverage percentages under all three simulation designs are very close to the true level of the corresponding confidence interval.

5. Analysis of the power usage data

The data shown in Figure 1b consist of daytime hourly power usage of a building from 9am to 4pm ($n = 8$ observations in a day) on $N = 44$ business days in June and July 2009. For the same days and hours we also have available the temperature at a local weather station. We apply our proposed methodology to these data treating each day as a replicate and modelling power usage as arising from $J = 2$ functions, one function giving power usage when the chiller is off ($j = 1$), and the other function giving power usage when the chiller is on ($j = 2$). In Section 5.1 we present the results assuming the covariance matrix \mathbf{V} is diagonal and in Section 5.2 we present the results when we assume \mathbf{V} is generated by the non-homogeneous random intercept model as in (3).

5.1. Results: diagonal \mathbf{V}

In this section we consider two models for \mathbf{V} : $\mathbf{V} = \sigma^2 \mathbf{I}$ and $\mathbf{V} = \mathbf{V}_{\mathbf{z}_k} = \text{diag}(\sigma_{z_{1k}}^2, \dots, \sigma_{z_{nk}}^2)$. We use the ECM algorithm described in Section 3.2 to estimate the model parameters considering *iid* z_{ik} s, Markov z_{ik} s and z_{ik} s that are independent with distribution depending on temperature. The smoothing parameters, the λ_j s, are chosen by cross-validation as described in detail in Section 3.3.

Figures 3a and 3b present the fitted functions for *iid* hidden states z_{ik} s when we assume $\mathbf{V} = \sigma^2 \mathbf{I}$ and $\mathbf{V}_{\mathbf{z}_k}$, respectively. We can observe that the fitted curves are very similar in the two figures. The estimated curve giving power usage when the chiller is on, obtained assuming $\mathbf{V} = \sigma^2 \mathbf{I}$, is slightly smoother than the one obtained assuming $\mathbf{V}_{\mathbf{z}_k}$. Table 2 presents the parameter estimates and chosen λ_j s. We can see that the estimates of $p_j = p(z_{ik} = j)$ from the two models for \mathbf{V} agree within the reported standard errors. We also observe in the lower half of the Table that the estimated variance when the chiller is on is much higher than when the chiller is off.

Figures 3c and 3d present the fitted curves for Markov z_{ik} s when we assume $\mathbf{V} = \sigma^2 \mathbf{I}$ and $\mathbf{V}_{\mathbf{z}_k}$, respectively. As in the *iid* case, the fitted curve giving power usage when the chiller is on obtained assuming $\mathbf{V} = \sigma^2 \mathbf{I}$ is slightly smoother than the one obtained assuming $\mathbf{V}_{\mathbf{z}_k}$. Table 3 provides information on the estimated model parameters and the chosen smoothing parameters. As in the *iid* case, the estimated variance when the chiller is on is much higher than when the chiller is off. We observe that the estimates of a_{21} , the transition probability

from “chiller on” to “chiller off”, are very small or equal to zero. Any estimate of a_{21} is expected to be small, as there is only one replicate in the data set where we observe this transition. The estimate of zero is reasonable when we assume different variances; \hat{a}_{21} is zero because the transition happens gradually, which our model does not allow, and the method incorrectly classifies all observations as coming from the condition “chiller on”, failing to detect the transition. This replicate is the green curve in Figure 3d.

Figure 4a presents the fitted curves when we assume the z_{ik} s are independent with the distribution of z_{ik} depending on temperature via the following logistic regression model:

$$\log \frac{p(\text{chiller on} \mid \text{temperature})}{p(\text{chiller off} \mid \text{temperature})} = \beta_0 + \beta_1 \text{ temperature}.$$

Table 4 shows the corresponding estimated model parameters assuming \mathbf{V}_{z_k} along with the chosen smoothing parameters, the λ_j s. We observe in Table 4 that the standard error for $\hat{\beta}_1$ is very small and by considering a confidence interval of the form $\hat{\beta}_1 \pm 1.96 \times \text{SE}(\hat{\beta}_1)$ we conclude that the coefficient β_1 is statistically significant.

5.2. Results: correlated observations generated by the non-homogeneous random intercept model

In the analyses of Section 5.1, we see that the variability in energy consumption when the chiller is on is higher than when the chiller is off. Thus, models such as $\mathbf{V} = \sigma^2 \mathbf{I}$ or \mathbf{V} following the homogeneous random intercept model may not be appropriate. Therefore, to model this heterogeneity in variance and the correlation between observations, we fit the proposed switching nonparametric regression model to the power usage data assuming the covariance matrix \mathbf{V} is generated by the non-homogeneous random intercept model as in (3). We use the ECM algorithm described in Section 3 and in Section 1.2 of the Supplementary Material to obtain the parameter estimates. We conduct the analysis assuming the hidden states z_{ik} s are *iid*. We assume that $\lambda_1 = \lambda_2 = \lambda$ and choose the smoothing parameters via a “brute force” leave-one-curve-out method over a grid of possible values of λ (see Table 1 of Supplementary Material).

Table 5 presents the parameter estimates. We observe that the estimates of p_1 and p_2 in Table 5 agree within the reported standard errors with the estimates obtained in Table 2 where we assume the observations are uncorrelated. Figure 4b shows the corresponding fitted curves. We can observe that the fitted function corresponding to the condition “chiller on” is lower than that in Figures 3a to 4a. The non-homogeneous random intercept model appears to “explain” days of high power usage by a larger variability of the “chiller on” random intercept. Thus the replicates with very high power usage have less of an impact on the final fitted “chiller on” curve.

6. Discussion

We have introduced a method for the analysis of data arising from random samples of a process with a complex structure. The structure depends on a latent state process where each state corresponds to a true smooth regression function. The estimation techniques and standard error calculations were developed for several specific cases of state processes and error covariances. We have considered restrictive covariance structures, save for the case where \mathbf{V} is completely unrestricted. While the covariance models we consider may not capture all of the dependencies in a data set, our techniques and ideas should carry over to more complex time series modelling of the error process. For instance, we can model more complicated covariance structures via random regression approaches, such as with B-spline basis functions or with lines that have random slopes in addition to random intercepts. Similarly, we can use our methods to consider more complex models for the latent process, such as a Markov model with covariate-dependent transition probabilities. Further useful extensions might incorporate a dependence among replicates; for instance, in studying energy consumption of several buildings, one would want to incorporate a random “building” effect.

Acknowledgements

We would like to thank the Editor, Associate Editor and reviewers for their insightful questions and comments.

References

- BROWN, M., BARRINGTON-LEIGH, C. and BROWN, Z. (2012). Kernel regression for real-time building energy analysis. *Journal of Building Performance Simulation* **5** 263–276.
- CAPPÉ, O., MOULINES, E. and RYDÉN, T. (2005). *Inference in Hidden Markov Models*. Springer Verlag.
- DE SOUZA, C. P. E. and HECKMAN, N. E. (2014). Switching nonparametric regression models. *Journal of Nonparametric Statistics* **26** 617–637.
- DEMPSTER, A. P., LAIRD, N. M. and RUBIN, D. B. (1977). Maximum likelihood from incomplete data via the EM algorithm. *Journal of the Royal Statistical Society Series B* **39** 1–38.
- JAMES, G. M., HASTIE, T. J. and SUGAR, C. A. (2000). Principal component models for sparse functional data. *Biometrika* **87** 587–602.
- LANGROCK, R., KNEIB, T., GLENNIE, R. and MICHELOT, T. (2017). Markov-switching generalized additive models. *Statistics and Computing* **27** 259–270.
- LOUIS, T. A. (1982). Finding the observed information matrix when using the EM algorithm. *Journal of the Royal Statistical Society Series B* **44** 226–233.
- MACDONALD, I. L. (2014). Numerical Maximisation of Likelihood: A Neglected Alternative to EM? *International Statistical Review* **82** 296–308.

- MCLACHLAN, G. J. and KRISHNAN, T. (2008). *The EM Algorithm and Extensions*. 2nd Ed., Wiley New York.
- MENG, X. L. and RUBIN, D. B. (1993). Maximum likelihood estimation via the ECM algorithm: a general framework. *Biometrika* **80** 267-278.
- OU, X. and MARTIN, E. (2008). Batch process modelling with mixtures of Gaussian processes. *Neural Computing & Applications* **17** 471-479.
- RAMSAY, J. O. and SILVERMAN, B. (2005). *Functional Data Analysis*. Springer Verlag.
- RASMUSSEN, C. E. and GHAHRAMANI, Z. (2002). Infinite mixtures of Gaussian process experts. In *Advances in Neural Information Processing Systems 14: Proceedings of the 2001 Conference* **2** 881-888. The MIT Press.
- TRESP, V. (2001). Mixtures of Gaussian processes. In *Advances in Neural Information Processing Systems 13: Proceedings of the 2000 Conference* 654-660. The MIT Press.
- WAHBA, G. (1990). *Spline models for observational data* **59**. Siam.
- YAO, F., MÜLLER, H.-G. and WANG, J.-L. (2005). Functional data analysis for sparse longitudinal data. *Journal of the American Statistical Association* **100** 577-590.
- ZUCCHINI, W., MACDONALD, I. L. and LANGROCK, R. (2016). *Hidden Markov models for time series: an introduction using R, 2nd Edition*. Chapman and Hall/CRC.

Appendix

Proof of Theorem 1

Theorem 1 is based on the following lemmas, which frame the problem for fixed j and fixed λ (so these are dropped in notation) and with general matrices \mathcal{W}_r , $r = 1, \dots, N$. Lemma 1 holds for general penalties, while Lemma 2 places further restrictions, restrictions that hold in our setting. Throughout, we assume that all maximizers exist.

Let $\hat{f}^{(-k)}$ maximize

$$S^{(-k)}(f) = -\frac{1}{2} \sum_{r=1; r \neq k}^N [\mathbf{y}_r - f(\mathbf{x})]^T \mathcal{W}_r [\mathbf{y}_r - f(\mathbf{x})] + P(f).$$

Lemma 1 Let $\hat{f}^{(*k)}$ maximize

$$\begin{aligned} S^{(*k)}(f) &= -\frac{1}{2} [\hat{f}^{(-k)}(\mathbf{x}) - f(\mathbf{x})]^T \mathcal{W}_k [\hat{f}^{(-k)}(\mathbf{x}) - f(\mathbf{x})] \\ &\quad -\frac{1}{2} \sum_{r=1, r \neq k}^N [\mathbf{y}_r - f(\mathbf{x})]^T \mathcal{W}_r [\mathbf{y}_r - f(\mathbf{x})] + P(f). \end{aligned}$$

If \mathcal{W}_k is positive definite then $\hat{f}^{(-k)}(\mathbf{x}) = \hat{f}^{(*k)}(\mathbf{x})$.

Proof of Lemma 1.

For simplicity let $k = 1$. We want to show that $\hat{f}^{(-1)} = \hat{f}^{(*1)}$. We know $\hat{f}^{(-1)}$ maximizes $S^{(-1)}(f)$ and, therefore,

$$S^{(-1)}(\hat{f}^{(-1)}) - S^{(-1)}(\hat{f}^{(*1)}) \geq 0.$$

We also know that $\hat{f}^{(*1)}$ maximizes $S^{(*1)}(f)$. Thus, $S^{(*1)}(\hat{f}^{(*1)}) - S^{(*1)}(\hat{f}^{(-1)}) \geq 0$, that is,

$$\begin{aligned} & -\frac{1}{2} [\hat{f}^{(-1)}(\mathbf{x}) - \hat{f}^{(*1)}(\mathbf{x})]^T \mathcal{W}_1 [\hat{f}^{(-1)}(\mathbf{x}) - \hat{f}^{(*1)}(\mathbf{x})] \\ & -\frac{1}{2} \sum_{r=2}^N [\mathbf{y}_r - \hat{f}^{(*1)}(\mathbf{x})]^T \mathcal{W}_r [\mathbf{y}_r - \hat{f}^{(*1)}(\mathbf{x})] + P(\hat{f}^{(*1)}) \\ & +\frac{1}{2} \sum_{r=2}^N [\mathbf{y}_r - \hat{f}^{(-1)}(\mathbf{x})]^T \mathcal{W}_r [\mathbf{y}_r - \hat{f}^{(-1)}(\mathbf{x})] - P(\hat{f}^{(-1)}) \geq 0, \end{aligned}$$

such that

$$-\frac{1}{2} [\hat{f}^{(-1)}(\mathbf{x}) - \hat{f}^{(*1)}(\mathbf{x})]^T \mathcal{W}_1 [\hat{f}^{(-1)}(\mathbf{x}) - \hat{f}^{(*1)}(\mathbf{x})] \geq S^{(-1)}(\hat{f}^{(-1)}) - S^{(-1)}(\hat{f}^{(*1)}) \geq 0,$$

which implies that

$$[\hat{f}^{(-1)}(\mathbf{x}) - \hat{f}^{(*1)}(\mathbf{x})]^T \mathcal{W}_1 [\hat{f}^{(-1)}(\mathbf{x}) - \hat{f}^{(*1)}(\mathbf{x})] \leq 0,$$

and, because \mathcal{W}_1 is positive definite, $\hat{f}^{(-1)}(\mathbf{x}) = \hat{f}^{(*1)}(\mathbf{x})$. \square

Lemma 2 Suppose that \mathcal{W}_k is positive definite for $k = 1, \dots, N$. Let \hat{f} maximize

$$S(f) = -\frac{1}{2} \sum_{k=1}^N [\mathbf{y}_k - f(\mathbf{x})]^T \mathcal{W}_k [\mathbf{y}_k - f(\mathbf{x})] + P(f).$$

If there exist matrices \mathcal{H}_k , $k = 1, \dots, N$, not depending on the \mathbf{y}_r s, such that $\hat{f}(\mathbf{x}) = \sum_{k=1}^N \mathcal{H}_k \mathbf{y}_k$, then

$$(\mathbf{I} - \mathcal{H}_k) [\hat{f}^{(-k)}(\mathbf{x}) - \mathbf{y}_k] = \hat{f}(\mathbf{x}) - \mathbf{y}_k.$$

Proof of Lemma 2

Note that $\hat{f}^{(*k)}$, as defined in Lemma 1, is the maximizer of S with \mathbf{y}_k replaced by $\hat{f}^{(-k)}$. By the assumption of the form of the maximizer of S , $\hat{f}^{(*k)}(\mathbf{x})$ can be written as

$$\begin{aligned} \hat{f}^{(*k)}(\mathbf{x}) &= \sum_{r=1:r \neq k}^N \mathcal{H}_r \mathbf{y}_r + \mathcal{H}_k \hat{f}^{(-k)}(\mathbf{x}) \\ &= \hat{f}(\mathbf{x}) - \mathcal{H}_k \mathbf{y}_k + \mathcal{H}_k \hat{f}^{(-k)}(\mathbf{x}). \end{aligned}$$

From Lemma 1 we know $\hat{f}^{(-k)}(\mathbf{x}) = \hat{f}^{(*k)}(\mathbf{x})$. Thus,

$$\hat{f}^{(-k)}(\mathbf{x}) = \hat{f}(\mathbf{x}) - \mathcal{H}_k \mathbf{y}_k + \mathcal{H}_k \hat{f}^{(-k)}(\mathbf{x}).$$

Now subtracting \mathbf{y}_k from both sides of this equation, we obtain

$$(\mathbf{I} - \mathcal{H}_k)[\hat{f}^{(-k)}(\mathbf{x}) - \mathbf{y}_k] = \hat{f}(\mathbf{x}) - \mathbf{y}_k.$$

□

TABLE 1

Simulation study. The mean and the standard deviation (SD) of the estimates of the parameters of the latent state process under each design, along with the mean of our proposed standard errors (SEs) and empirical coverage percentages of the proposed confidence intervals.

| Design | true parameters | confidence intervals | | empirical coverage | |
|--------|-----------------|----------------------|-------------|--------------------|-------|
| | | mean (SD) | mean of SEs | 90% | 95% |
| 1 | $p_1 = 0.5$ | 0.499 (0.016) | 0.016 | 90.3% | 95.7% |
| 2 | $\pi_1 = 0.5$ | 0.502 (0.050) | 0.050 | 89.7% | 95.7% |
| | $a_{12} = 0.3$ | 0.300 (0.021) | 0.020 | 90.0% | 94.3% |
| | $a_{21} = 0.4$ | 0.401 (0.024) | 0.025 | 89.7% | 95.3% |
| 3 | $\beta_0 = 2$ | 2.010 (0.173) | 0.177 | 91.0% | 96.7% |
| | $\beta_1 = 5$ | 5.047 (0.357) | 0.364 | 90.7% | 94.3% |

TABLE 2

Data analysis results for iid z_{ik} s for $\mathbf{V} = \sigma^2 \mathbf{I}$ and $\mathbf{V}_{\mathbf{z}_k} = \text{diag}(\sigma_{z_{1k}}^2, \dots, \sigma_{z_{nk}}^2)$, with corresponding fitted curves in Figures 3a and 3b, respectively. Note that for $\mathbf{V} = \sigma^2 \mathbf{I}$ the estimate $\hat{\sigma}^2$ does not depend on j and, therefore, its value appears in the middle row.

| | curve (chiller condition, j) | $\hat{\sigma}_j^2$ | \hat{p}_j (SE) | λ_j |
|--|---------------------------------|--------------------|------------------|-------------|
| $\mathbf{V} = \sigma^2 \mathbf{I}$ | black (off, $j = 1$) | 103.5 | 0.665 (0.025) | 0.020 |
| | red (on, $j = 2$) | | 0.335 (0.025) | 0.078 |
| $\mathbf{V}_{\mathbf{z}_k} = \text{diag}(\sigma_{z_{1k}}^2, \dots, \sigma_{z_{nk}}^2)$ | black (off, $j = 1$) | 12.7 | 0.658 (0.025) | 0.073 |
| | red (on, $j = 2$) | 355.4 | 0.342 (0.025) | 0.006 |

TABLE 3

Data analysis results for Markov z_{ik} s, for $\mathbf{V} = \sigma^2 \mathbf{I}$ and $\mathbf{V}_{\mathbf{z}_k} = \text{diag}(\sigma_{z_{1k}}^2, \dots, \sigma_{z_{nk}}^2)$, with corresponding fitted curves in Figures 3c and 3d. Note that for $\mathbf{V} = \sigma^2 \mathbf{I}$ the estimate $\hat{\sigma}^2$ does not depend on j and, therefore, its value appears in the middle row. In addition, for the case when $\mathbf{V}_{\mathbf{z}_k} = \text{diag}(\sigma_{z_{1k}}^2, \dots, \sigma_{z_{nk}}^2)$ we are not able to obtain SEs for $\hat{\pi}_1, \hat{\pi}_2, \hat{a}_{12}$ and \hat{a}_{21} as $\hat{a}_{21} < 10^{-16}$.

| | curve (chiller condition, j) | $\hat{\sigma}_j^2$ | $\hat{\pi}_j$ (SE) | \hat{a}_{12} (SE) | \hat{a}_{21} (SE) | λ_j |
|--|---------------------------------|--------------------|--------------------|---------------------|---------------------|-------------|
| $\mathbf{V} = \sigma^2 \mathbf{I}$ | black (off, $j = 1$) | 103.4 | 0.705 (0.069) | 0.024 | 0.00991 | 0.019 |
| | red (on, $j = 2$) | | 0.295 (0.069) | (0.011) | (0.00986) | 0.083 |
| $\mathbf{V}_{\mathbf{z}_k} = \text{diag}(\sigma_{z_{1k}}^2, \dots, \sigma_{z_{nk}}^2)$ | black (off, $j = 1$) | 12.2 | 0.682 | 0.015 | $< 10^{-16}$ | 0.049 |
| | red (on, $j = 2$) | 400.1 | 0.318 | - | - | 0.006 |

TABLE 4

Data analysis results for z_{ik} s with distribution depending on a covariate (temperature) and $\mathbf{V}_{\mathbf{z}_k} = \text{diag}(\sigma_{z_{1k}}^2, \dots, \sigma_{z_{nk}}^2)$ with corresponding fitted curves in Figure 4a.

| | curve (chiller condition, j) | $\hat{\sigma}_j^2$ | $\hat{\beta}$ (SE) | λ_j |
|--|---------------------------------|--------------------|-----------------------------------|-------------|
| | black (off, $j = 1$) | 17.9 | $\hat{\beta}_0 = -13.013$ (1.411) | 0.115 |
| | red (on, $j = 2$) | 274.0 | $\hat{\beta}_1 = 0.607$ (0.068) | 0.030 |

TABLE 5
 Data analysis results for iid z_{ik} s and \mathbf{V} depending on the hidden states generated by a non-homogeneous random intercept model with $\lambda_1 = \lambda_2 = 0.1$ chosen via cross-validation and corresponding curves in Figure 4b. Note that $\hat{\sigma}^2$, $\hat{\tau}_1^2$ and $\hat{\tau}_2^2$ do not depend on j .

| curve (chiller condition, j) | $\hat{\sigma}^2$ | $\hat{\tau}_1^2$ | $\hat{\tau}_2^2$ | \hat{p}_j (SE) |
|---------------------------------|------------------|------------------|------------------|------------------|
| black (off, $j = 1$) | 14.9 | 11.0 | 505.0 | 0.662 (0.025) |
| red (on, $j = 2$) | | | | 0.338 (0.025) |

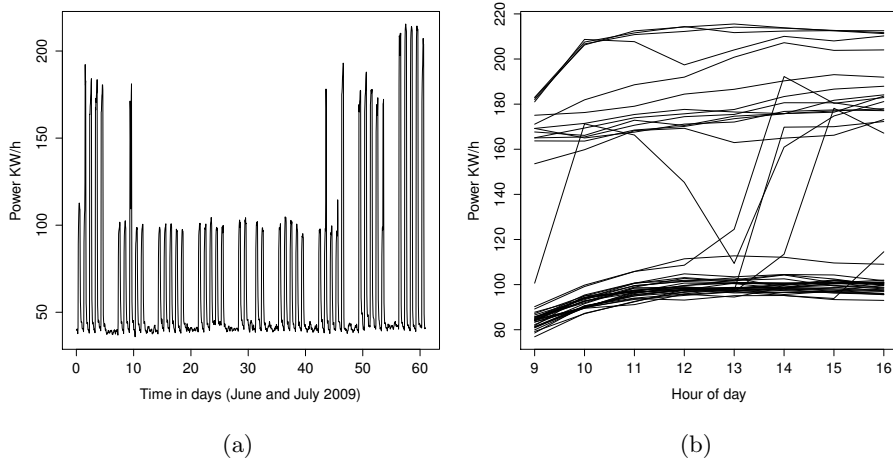
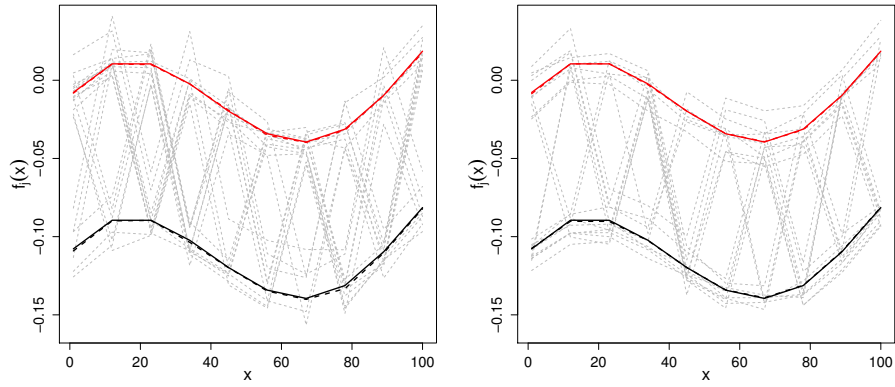
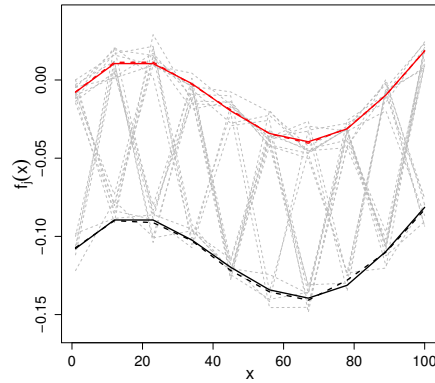


Fig 1 (a) Power usage in June and July 2009 in a building monitored by Pulse Energy. (b) Daytime power usage from 9am to 4pm on business days (each curve corresponds to a different day) in June and July 2009 for the same building.



(a) Design 1: iid z_{iks}

(b) Design 2: Markov z_{iks}



(c) Design 3: covariate dependent z_{iks}

Fig 2 Example of simulated data along with $\hat{f}_1(\mathbf{x})$ and $\hat{f}_2(\mathbf{x})$ for each simulation design. The gray dashed curves correspond to 20 out of the 100 generated replicates. The black and red solid curves correspond to the true functions f_1 and f_2 , respectively, evaluated only at \mathbf{x} . The black and red dashed curves correspond to $\hat{f}_1(\mathbf{x})$ and $\hat{f}_2(\mathbf{x})$, respectively.

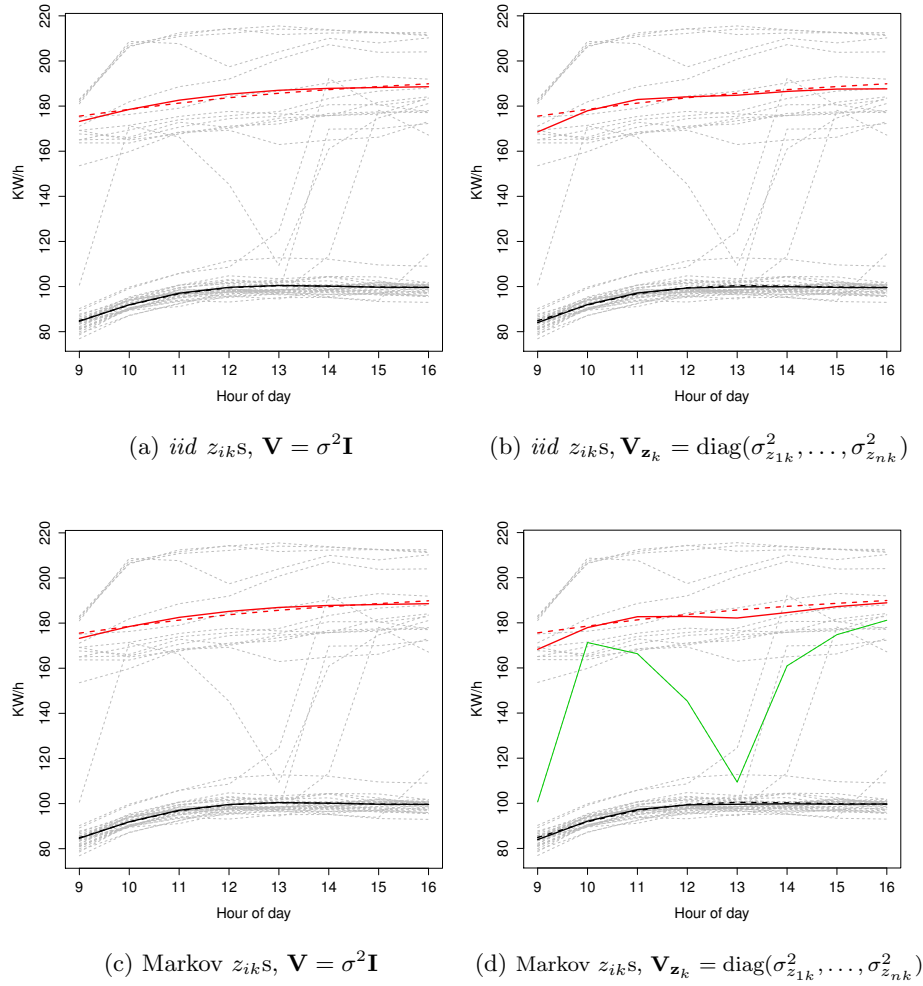


Fig 3 Building daytime power usage. Fitted function estimates (solid curves) assuming $iid\ z_{ik}S$ (top row) and Markov $z_{ik}S$ (bottom row). In (a) and (c) we consider $\mathbf{V} = \sigma^2 \mathbf{I}$. In (b) and (d) $\mathbf{V}_{z_k} = \text{diag}(\sigma_{z_{1k}}^2, \dots, \sigma_{z_{nk}}^2)$. The gray dashed curves correspond to the replicates. The red and black dashed curves are the initial function estimates. The colors red and black correspond to the condition chiller on and off, respectively. The green curve in (d) corresponds to the replicate where there is a transition from chiller on to off.

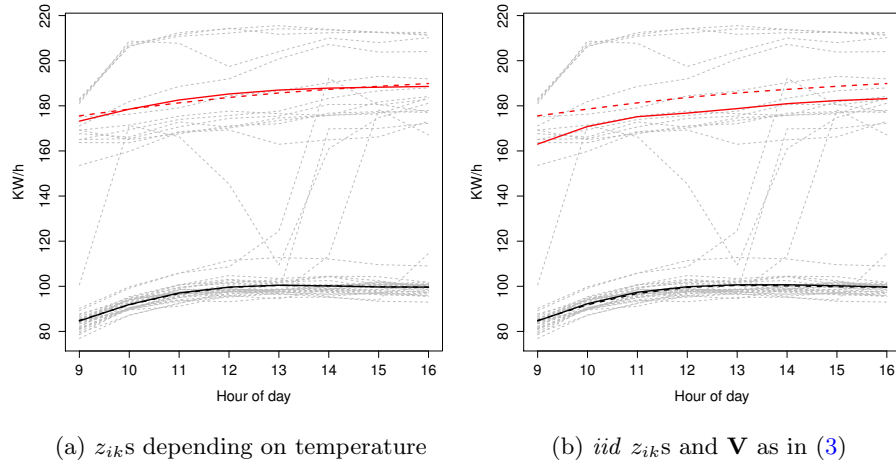


Fig 4 Building daytime power usage. (a) Fitted function estimates assuming the z_{ik} s are independent with distribution depending on temperature. $\mathbf{V}_{z_k} = \text{diag}(\sigma_{z_{1k}}^2, \dots, \sigma_{z_{nk}}^2)$. (b) Fitted function estimates assuming *iid* z_{ik} s and \mathbf{V} generated by a non-homogeneous random intercept model as in (3). Components of the plots are as in Figure 3a.